

Authors' response to RC1 (Alexander Schaaf's) interactive comment on "Uncertainty assessment for 3D geologic modeling of fault zones based on geologic inputs and prior knowledge".

5 Reviewer's comments are shown in italicized fonts, and the authors' responses and changes to the manuscript are highlighted with callouts. The general comments are shown and addressed first, then the specific comments are addressed by line/figure number.

1 General comments

10 *The paper presents a step forward in the uncertainty-aware modeling of subsurface faults in structural geomodels. The authors make use of Monte Carlo simulations to simulate uncertainty of fault zones based on a specific fault zone parameterization (surface traces, vertical termination surfaces, structural orientation and fault zone thickness) using a proprietary software suite. The authors elaborate the use of anisotropic spherical distributions for parameterizing orientation data for uncertainty simulation, which is a valuable contribution. The manuscript is overall well structured, except for a few re-arrangements necessary to increase readability (detailed in the specific comments). The authors give proper credit to related work and clearly indicate their own contribution. The title clearly reflects the contents of the paper. The figures presented will require some work to improve legibility and to avoid confusion of the reader.*

20 *But the authors appear to be confusing their simulation approach: They introduce MCUP (i.e. Monte Carlo simulation) in the methodology and properly parameterize their stochastic geomodel using probability distributions. But they then erroneously describe that they use Markov Chain Monte Carlo (MCMC) sampling. MCMC sampling is used for exploring the posterior space, which does not exist in a Monte Carlo simulation (i.e. MCUP). As the probability space is known in a Monte Carlo simulation, it needs no exploration. In a Monte Carlo simulation we only don't know how the combination of samples effect the output of the simulator function (the geomodeling software), thus we randomly sample (Monte Carlo sampling) from the parameter distributions to create a geomodel ensemble that shows us how the uncertainty in the input parameters effects the geomodel output. Luckily, to my knowledge, the used probabilistic programming framework pymc3 defaults to Monte Carlo sampling when no likelihood function is given (and thus no Bayesian inference can be conducted). Thus the authors appear to have accidentally conducted the simulations they wanted to do (MCUP/Monte Carlo sampling). The use of trace plots (as in Figure 6 and 8) for Monte Carlo simulation results is meaningless though (and potentially misleading), as no sampler is being used that requires determination of convergence. As, luckily, the presented simulation results appear to be valid MCUP results, the authors only need to change their writing accordingly, without the need for re-running simulations.*

30 *In its current state, mixing up the terminology of Bayesian inference and MCUP, I can not recommend the paper to be accepted. But if the authors fix their method descriptions and discussions of the results to fit the MCUP simulations they actually conducted, I believe this could become a valid scientific contribution that is worth publishing in Solid Earth.*

35 Authors' answer:

The authors truly appreciate the detailed clarifying comments, especially regarding the description of the simulation approach. The authors acknowledge that there was confusion regarding how the simulation approach was described, primarily in the erroneous usage of the term Markov Chain Monte Carlo (MCMC) when the method applied in the study is in fact simply Monte Carlo sampling to explore the set of input probability distributions. The authors wish to reaffirm that the methodology employed in the study is intended to be that which the reviewer identified: the use of Monte Carlo sampling to explore the prior uncertainty space of geologic modeling inputs. As is, the analysis performed in the study does not contain any use of Bayesian inference via MCMC (i.e., no likelihood functions were defined or used), nor was this an intended description of the methodology employed. The authors have taken steps throughout the text to remove any erroneous descriptions of the methodology and clarify the intended use of Monte Carlo sampling. A broad overview of the changes made to rectify this error include (i) removal of any mention of MCMC or posterior distributions and replacement with appropriate terminology and (ii)

the removal of trace plots and a rethinking of the simulation quality assessment section.

2 Specific comments

50 2.1 1 - Introduction

2.1.1 *The Introduction of the paper needs to clearly state the scope of the study / hypothesis to be tested or explored.*

Authors' answer:

55 The two paragraphs previously in lines 52-68 have been incorporated fluidly into the introduction to specify the scope and motivation of the study.

Changes to the manuscript:

60 **Text moved to the end of Section 1 – Introduction. . .** This study expands the use of MCUP probabilistic geomodeling to a new aspect of geologic modeling – fault zones, or the localized volume of fractured and displaced rock surrounding a finite fault surface, typically composed of a fault core and a damage zone (Caine et al., 1996; Childs et al., 2009; Peacock et al., 2016; Choi et al., 2016). Fault zones introduce regions of altered geotechnical strength and hydraulic permeability into the surrounding in-tact rockmass and are therefore of major importance to geological engineering projects that rely on accurate assessments of subsurface rock properties (e.g., tunnels, mines). While faults have been the focus of a significant amount of recent geologic modeling research (Røe et al., 2014; Cherpeau et al., 2010; Cherpeau and Caumon, 2015; Aydin and Caers, 2017), these works have focused on modeling fault surfaces directly rather than modeling the 3D geometry of fault zones. Detailed modeling of the 3D geometry of fault zones can improve the understanding of faults' impacts on geotechnical and reservoir engineering projects due to the fact that variations in fault zone thickness or composition can greatly alter the mechanical and hydrological behavior of a fault, e.g., its sealing potential (Caine et al., 1996; Fredman et al., 2008; Manzocchi et al., 2010). ~~By an in-depth search of the literature, as of yet there is no dedicated approach to characterizing the uncertainty of fault zones in 3D geologic models.~~ Building on the existing literature on understanding the uncertainties about faults in the subsurface (Choi et al., 2016; Shipton et al., 2019; Torabi et al., 2019b), this study develops a novel, dedicated approach to leveraging probabilistic geomodeling to characterize the uncertainty of fault zones using 3D geologic models.

70 Fault zones may be irregular in shape, creating complex geometries which are difficult to characterize quantitatively (Torabi et al., 2019a, b). Peacock et al. (2016) provide a detailed list of the various types of damage zones and intersecting fault networks that comprise the general term “fault zone”. ~~The inherent complexity of fault zone structure makes their precise modeling intractable in an automated MCUP formulation.~~ The inherent complexity of fault zone structure makes their precise modeling intractable in an automated geologic modeling application, such as that required by probabilistic geomodeling. A simplified approach to modeling fault zones in 3D geologic models is developed in this study based on the key elements defining fault zone geometry at a practical level of detail.

2.2 2 - Model implementation

2.2.1 *L52 - Both paragraph (lines 52-68) need to be incorporated into the introduction as they define the scope and motivation of the study.*

Authors' answer:

85 See above comment regarding reorganizing the content of the Introduction.

2.3 3 - Probability distributions for MCUP

2.3.1 *L138 - How do you evaluate the likelihood of the proposal step in a Markov Chain during MCUP? This is only possible when doing a Bayesian inference, not a Monte Carlo uncertainty propagation, as you don't have any likelihood function.*

Authors' answer:

The erroneous mention of MCMC sampling algorithms has been removed and edited to specify the use of Monte Carlo sampling algorithms. This eliminates the question of "How do you evaluate the likelihood of the proposal step in a Markov Chain during MCUP?" by clarifying that only Monte Carlo sampling is performed, and not Bayesian inference.

Changes to the manuscript:

~~Simulation of scalar data is straightforward and well-established through the use of Markov-chain Monte Carlo (MCMC) sampling algorithms, easily accessible through the open source Python package *PyMC3* (Salvatier et al., 2016).~~ **Simulation of scalar data is straightforward and well-established through the use of Monte Carlo sampling algorithms, easily accessible through the open source Python package *PyMC3* (Salvatier et al., 2016).**

2.3.2 *Overall the description of simulation/sampling should be moved into Section 3.2.*

Authors' answer:

The description of simulation and sampling has been incorporated into Section 3.2.

Changes to the manuscript:

The paragraph referenced has been moved to Section 3.2: **Simulation of scalar data is straightforward and well-established through the use of Markov-chain Monte Carlo (MCMC) sampling algorithms, easily accessible through the open source Python package *PyMC3* (Salvatier et al., 2016). The *PyMC3* library has been demonstrated as a platform for performing MCUE of 3D geologic models (de la Varga and Wellmann, 2016; Schneeberger et al., 2017), and has even been implemented in the open source geologic modeling platform GemPy (de la Varga et al., 2019). An additional consideration in the case of continuous data types is the distinction between scalar and vectorial data (e.g., structural orientations). A probability distribution describing orientation data resides on the surface of a unit-sphere in 3D, and can be characterized using spherical probability distributions (Fisher et al., 1987; Mardia and Jupp, 2000). The benefit of using spherical probability distributions to describe structural orientation uncertainty in 3D geologic modeling is clearly stated by Pakyuz-Charrier et al. (2018b), and their application in MCUE formulations continues to develop (Pakyuz-Charrier et al., 2018b, a; Carmichael and Ailleres, 2016). To remain concise, the following section focuses on the new contributions made to the use of spherical probability distributions utilizing the *R-fast* open source package available in the R language (Papadakis et al., 2018).**

2.3.3 *L140 - The paper de la Varga & Wellmann (2016) uses pymc to conduct a Bayesian inference - thus not MCUP.*

Authors' answer:

While the referenced study in question includes the use of the MCUP approach for probabilistic geomodeling, the authors realize the lack of clarity due to the referenced paper's focus on *PyMC*'s capability to perform Bayesian inference. The sentence has been reworded and expanded to emphasize the capability of *PyMC3* to perform Monte Carlo sampling outside of a

130 Bayesian inference, fitting its application in the current study.

Changes to the manuscript:

135 The *PyMC3* library has been demonstrated as a platform for performing MCUP of 3D geologic models (de la Varga and Wellmann, 2016); and has even been implemented in the open-source geologic modeling platform GemPy (de la Varga et al., 2019). ~~The *PyMC3* library is designed to facilitate Bayesian inference using computational sampling algorithms, though the inclusion of likelihood functions is not required thereby allowing for utilization of the package functions for Monte Carlo sampling alone. The use of *PyMC3* has been demonstrated successfully in the context of 3D geologic modeling by de la Varga and Wellmann (2016); Schneeberger et al. (2017), and its implementation in *Theano* has allowed for seamless integration with the open source geologic modeling platform GemPy (de la Varga et al., 2019). This study focuses solely on the step of probabilistic geomodeling based on 3D geologic modeling inputs, leveraging only the Monte Carlo sampling capabilities of *PyMC3*.~~

2.4 3.2 - Simulation

2.4.1 *A more adequate name for the section would be “Sampling”.*

145 **Authors’ answer:**

The section name has been changed to Sampling.

2.5 3.3 - Rotation

2.5.1 *This section is part of sampling and should be merged into Section 3.2*

150 **Authors’ answer:**

The section has been appended to Section 3.2 - Sampling.

2.6 4.2 - Surface trace

2.6.1 *L291 - It is unclear to me what the “approximate geographical error of known landmarks” is.*

155 **Authors’ answer:**

The section containing this sentence has been revised and expanded to clearly define the sources of uncertainty affecting the fault trace and the methods with which they are quantified - including the geographical error arising from the use of a historic geologic map.

160

Changes to the manuscript:

165 The uncertainty affecting the surface fault trace results in changes in the trace location and shape. Independent perturbations of the trace’s endpoints are applied and linearly propagated along the fault trace to arrive at a smoothly varied location and shape. ~~A normal distribution characterizing the uncertainty about the location of each trace endpoint is parameterized from the joint uncertainty stemming from fault zone centerline definition, digitization error and geographical errors in addition to a random direction of shift obtained from a uniform distribution.~~ The three primary sources of uncertainty are quantified using the available information listed in respective order: average fault zone thickness, published metrological studies (Zhong-Zhong, 1995) and approximate geographical error of known landmarks (e.g., mountain tops). ~~Additional details on the method of~~

170 ~~perturbing the location and shape of the surface trace based on the joint effect of these sources of uncertainty are available in the code supplement.~~

175 A bounded uniform distribution is parameterized to simulate a random direction of perturbation for each trace endpoint due to geographical error (i.e., drafting and georeferencing error). The normal distribution representing the total bound on geographical error is converted to respective \hat{x} and \hat{y} components using the directional cosine of the angle sampled from the uniform distribution. This conversion to unit components is used similarly with the fault zone centerline definition uncertainty and digitization uncertainty using the acute angle θ between the orientation of the fault trace with the northing and easting directions. An additional logical check for the strike quadrant of the surface trace is required to implement this approach.

180 The individual sources of uncertainty affecting the surface trace endpoint locations are combined into a derived distribution using a deterministic function to determine the total uncertainty affecting the location of each endpoint, given by Eq. 1.

$$\begin{aligned} P(\hat{x}|\sigma_{centerline}, \sigma_{dig}, \sigma_{geo}, \theta) &= \cos(\theta) \left(N(0, \sigma_{centerline}) + N(0, \sigma_{dig}) \right) + N(0, \sigma_{geo}) \sin \left(U(0, 2\pi) \right), \\ P(\hat{y}|\sigma_{centerline}, \sigma_{dig}, \sigma_{geo}, \theta) &= \sin(\theta) \left(N(0, \sigma_{centerline}) + N(0, \sigma_{dig}) \right) + N(0, \sigma_{geo}) \cos \left(U(0, 2\pi) \right) \end{aligned} \quad (1)$$

185 The average fault zone thickness was used to characterize the fault zone centerline definition uncertainty affecting each surface trace endpoint. The geographical error was calculated to be approximately 40 meters based on the average distance measured between known landmarks (e.g., mountain tops) on the geologic map and modern satellite imagery data. For both of these sources of uncertainty, the maximum error range described is treated as a 95% confidence interval, allowing a normal distribution to be parameterized with a mean of zero and a standard deviation equal to $maximum\ error/3.92$. The digitization error for a 1:12,000 map was represented by a normal distribution with a standard deviation of 3.666 m based on (Zhong-Zhong, 1995).

190 2.7 4.3 - Vertical termination depth

2.7.1 *L312 - What is a deterministic distribution? Do you mean a derived distribution? Or an empirically parametrized distribution? A distribution should be by definitiv nondeterministic.*

Authors' answer:

195 The phrase "deterministic distribution" was used following the *PyMC3* function terminology `pm.Deterministic()`, which is used for combining multiple stochastic variables (i.e., distributions) using a deterministic function. As the reviewer notes, this function is in fact empirically parameterized, and the more appropriate name "empirically derived distribution" – also known as a deterministic model combining multiple stochastic variables in *PyMC3* terminology – has been substituted. The description of the use of this style of distribution has been modified to clarify the reliance on combining several stochastic variables using
200 an empirically derived deterministic function.

Changes to the manuscript:

205 ~~The vertical termination depth is sampled from a deterministic distribution combining uncertainty about the aspect ratio, fault trace persistence and prior information of the fault elevation and average dip. Sampling the uncertainty of the fault zone vertical termination depth involves combining multiple probability distributions using a deterministic function to generate an empirically derived probability distribution. In the derived distribution for fault zone vertical termination depth, f_{length} and $Aspectratio$ are characterized as independent probability distributions (respectively) and combined using a deterministic function based on the empirically derived description of 3D fault surface geometry, $z_{term} = z_{outcrop} - f_{height} * \sin(\theta)$; $f_{height} =$~~
210 $\frac{f_{length}}{Aspectratio}$. In this manner, the vertical termination depth (z_{term}) is calculated by converting the fault height to the vertical height using the average dip angle (θ) and subtracting this from the average elevation of the fault outcrop ($z_{outcrop}$).

2.8 4.5 - Simulation quality assessment

215 2.8.1 L334 - *Without a likelihood function you can't use a MCMC sampler, as you are unable to evaluate the step proposals.*

2.8.2 L336 - *In an MCUP simulation, you have no posterior uncertainty space, as you are not using any likelihood function. You are mixing up terminology of MCUP and Bayesian inference. Again, MCMC sampling is only possible with a likelihood function (thus not in MCUP).*

Authors' answer:

220 The entire Section 4.5 has been revised in depth to remove erroneous inclusions of the terminology MCMC sampler and to remove the erroneous use of trace plots in assessing the quality of Monte Carlo simulation for exploring the prior uncertainty space.

Changes to the manuscript:

225

The quality of probabilistic simulation ~~relies on primarily~~ **is a product of** the size of the uncertainty space, the simulation method **used** and the number of samples drawn. For any simulation, the realizations generated can be plotted in the data space and visually examined for appropriate coverage and shape (termed a realization plot). For ~~non-spherical~~ **scalar** data types, ~~use of MCMC simulation methods creates trace plots and posterior histograms~~ **of the Monte Carlo draws provide an intuitive method for independently assessing the quality of simulation for each input.** ~~, which provide an intuitive method for independently assessing the quality of simulation for each input. Uniformity of the trace plot and width of the 95% highest posterior density (HPD) indicate, respectively, the convergence of the Markov Chain sampling and the thorough exploration of the posterior uncertainty space.~~ **Visual analysis of the shape of the histogram compared to the expected shape of the distribution and a comparison between the input distribution parameters (e.g., mean and standard deviation for a normal distribution) and their values calculated from the samples can quickly determine whether the samples drawn have sufficiently explored the uncertainty space.** Figure 6 shows an example of the realization plot, ~~trace plots and posterior~~ **sample** histograms generated for the simulation of vertical termination depths from Section 4.3. This figure allowed for identifying a strong tailing behavior in the output realizations, leading to a reparameterization discussed in Section 6.2.

230

235

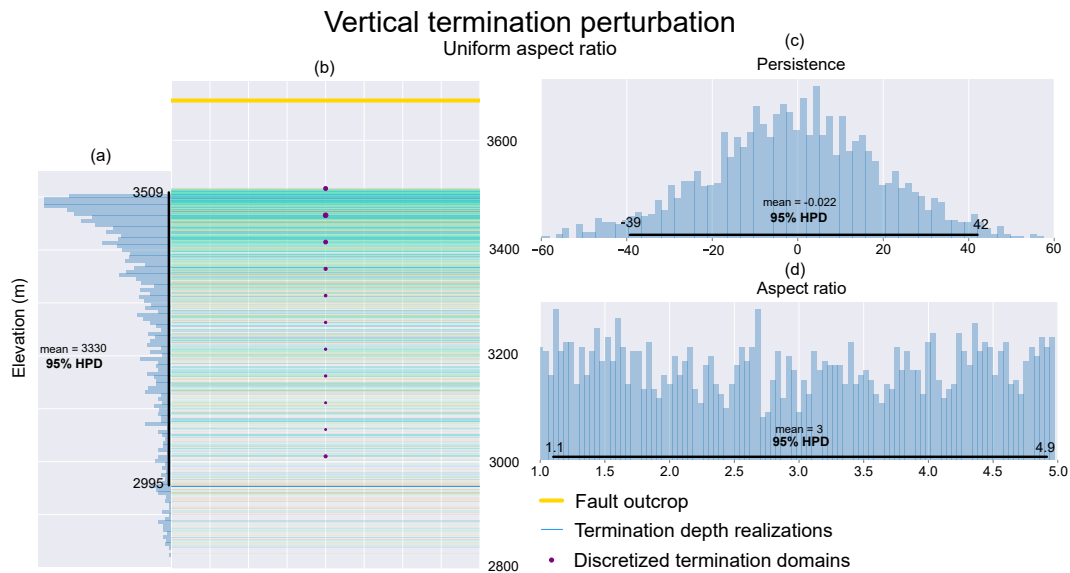


Figure 1. Realizations and Monte Carlo analysis results (trace plot and posterior histograms) **Visualization of Monte Carlo samples and associated geologic input realizations** from perturbation of the fault zone vertical termination depth based on a uniform distribution of fault aspect ratio. The 95% highest posterior predictive density is overlain on the posterior histograms of the Monte Carlo samples.

Trace plots are not available for the spherical data simulations due to reliance on the acceptance-rejection simulation method, while posterior **For spherical data simulations**, histograms may be replaced by Exponential Kamb contouring (Vollmer, 1995) or Rose diagrams to visualize the density of sampled poles across the surface of the unit sphere (as projected onto a lower-hemisphere projection). This visual assessment provides a semi-quantitative evaluation of the shape and distribution of the posterior spherical probability distribution **sampled structural orientations**. Additionally, a recalculation of the eigenvector decomposition from the set of simulated samples provides a measure of the accuracy of the posterior distribution with respect to the input orientation **parameter** values. Tools for generating figures for simulation quality assessment are provided and detailed in the input perturbation script.

Based on the assessment of simulation quality and consideration of compounding factors during uncertainty propagation, the MCUE formulation for the single fault model was run for a number of various realization counts (100, 300, 500, 1,000, 2,000 and 3,000). The processing time generally increases linearly with realization count, reaching many hours to several days for high realization counts on the single fault mock model containing 2.5 million cells. **The vast majority of processing time is taken up by the model updating and block model calculation in Leapfrog. For the single fault mock model with 1,000 realizations and 2.5 million cells the sampling benchmark time was 87 seconds while the model processing benchmark time was 38.5 hours.** This study is intended to introduce and expand on the use of MCUE formulations for specific geologic modeling problems, and work regarding optimizing the efficiency of model processing is not a focus. The experiments conducted do highlight the need to understand (i) the realization requirement for exploring modeling inputs independently and its relationship to the size of the independent uncertainty spaces, (ii) the interactions of various, related parameters during the uncertainty propagation step and (iii) identification of a balance between final model resolution, coverage, complexity and processing time.

2.9 6.2 - Model parameterization

2.9.1 L388 - The use of “posterior distribution” is false, as you are doing MCUP, not a Bayesian inference.

260 **Authors’ answer:**

In line with the general comments regarding erroneous usage of terms from Bayesian inference (MCMC, posterior distributions), the description here has been revised to appropriately describe the prior predictive model that was explored using Monte Carlo sampling.

265

Changes to the manuscript:

However, the posterior **empirically derived** distribution of vertical termination depths resulting from a bounded uniform parameterization of fault aspect ratio showed a strong tailing effect (right skewed).

270 **2.10 6.3 - Parameter relationships**

2.10.1 L411 - The meaning of the entire paragraph is unclear to me and needs to be revised.

Authors' answer:

275 The specified paragraph on addressing the observed relationships among geologic modeling input parameters using the MCUP formulation has been revised clarify the authors' stance on why and how these parameter relationships arise in the MCUP formulation. In essence, the paragraph is intended to highlight the potential for undersampling the geologic model uncertainty space when considering overlapping uncertainty envelopes of individual model inputs.

Changes to the manuscript:

280

Relationships between modeling inputs also arise in different ways, for example the vertical termination depth and structural orientation uncertainty envelopes overlap heavily in the combined model uncertainty (Figure 5) leading to undersampling of the model uncertainty space when the independent uncertainty envelopes are combined. Similar behavior is observed when comparing orientation perturbations to fault zone thickness where thinner fault zones require finer orientation perturbations to fully populate the uncertainty space of the 3D geologic model. **Despite performing a thorough exploration of each, independent parameter's uncertainty during Monte Carlo sampling (Section 4.5), undersampling of the combined geologic model uncertainty space can still occur during uncertainty propagation. An example of this arises when considering the vertical termination depth and structural orientation. Truncation of fault zone realizations at any given termination interval effectively reduces the number of realizations available for sampling the full range of structural orientation uncertainty at deeper intervals. This is evidenced in Figure 5(b) by the increasing prevalence of "stair-stepping" artefacts in the combined model uncertainty with depth.**

290

2.10.2 L419 - Gibbs sampling is not applicable to MCUP, as no likelihood is used.

Authors' answer:

295

The erroneous mention of Gibbs sampling has been removed. The section has been revised to better highlight the potential for exploring the input uncertainty space using joint distributions among various parameters believed to be correlated.

Changes to the manuscript:

300

A treatment of these relationships through ~~the use of Gibbs sampling or other conditional methods of Monte Carlo simulation~~ **parameterizing previously independent input probability distributions using a joint distribution (and an appropriate sampling scheme)** could potentially generate more realistic and efficient assessments of model uncertainty.

3 Figures

305 3.1 Figure 2

The dotted volume texture makes annotations for uncertainty extremely hard to read. The same goes for there fault zone signature/texture. I'd highly recommend removing as much texture as possible from the plot to improve legibility.

310 "The Visual Display of Quantitative Information" by Edward Tufte provides ample of additional reasons for reducing distracting "ink" from scientific visualizations and is well worth a read :-)

Authors' answer:

315 The suggested changes have been made to the fault zone schematic figure, clearing away non-informative ink and emphasizing the illustrated uncertainty envelopes. Thank you very much to the reviewer for the kind suggestion on better practices for graphical display.

Changes to the manuscript:

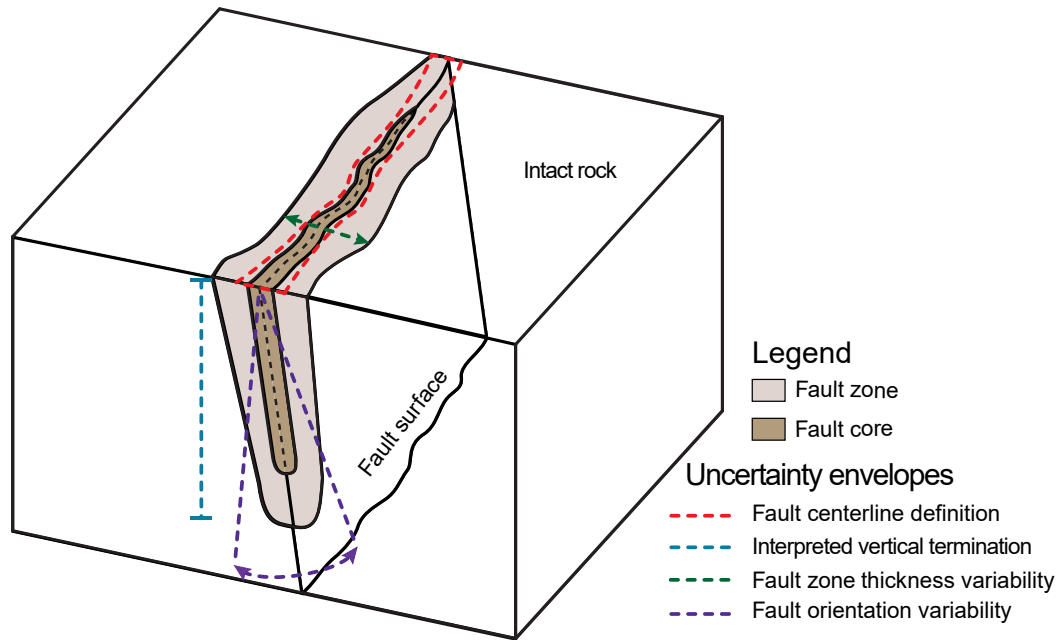


Figure 2. A schematic showing the sources of uncertainty possible uncertainty envelopes about the four geologic modeling inputs used to characterize the 3D geometry of a fault zone in the subsurface. Modified from Krajnovich et al. (2020).

320 3.2 Figure 4

Highlighting of fault traces is really difficult to see. I highly recommend making this figure more legible to the reader by removing visual complexity: e.g. remove coloring of geological map in the background.

Authors' answer:

325

The figure has been edited to make the fault traces bolder and to provide a stronger contrast between the fault traces and the geological map in the background.

Changes to the manuscript:

330

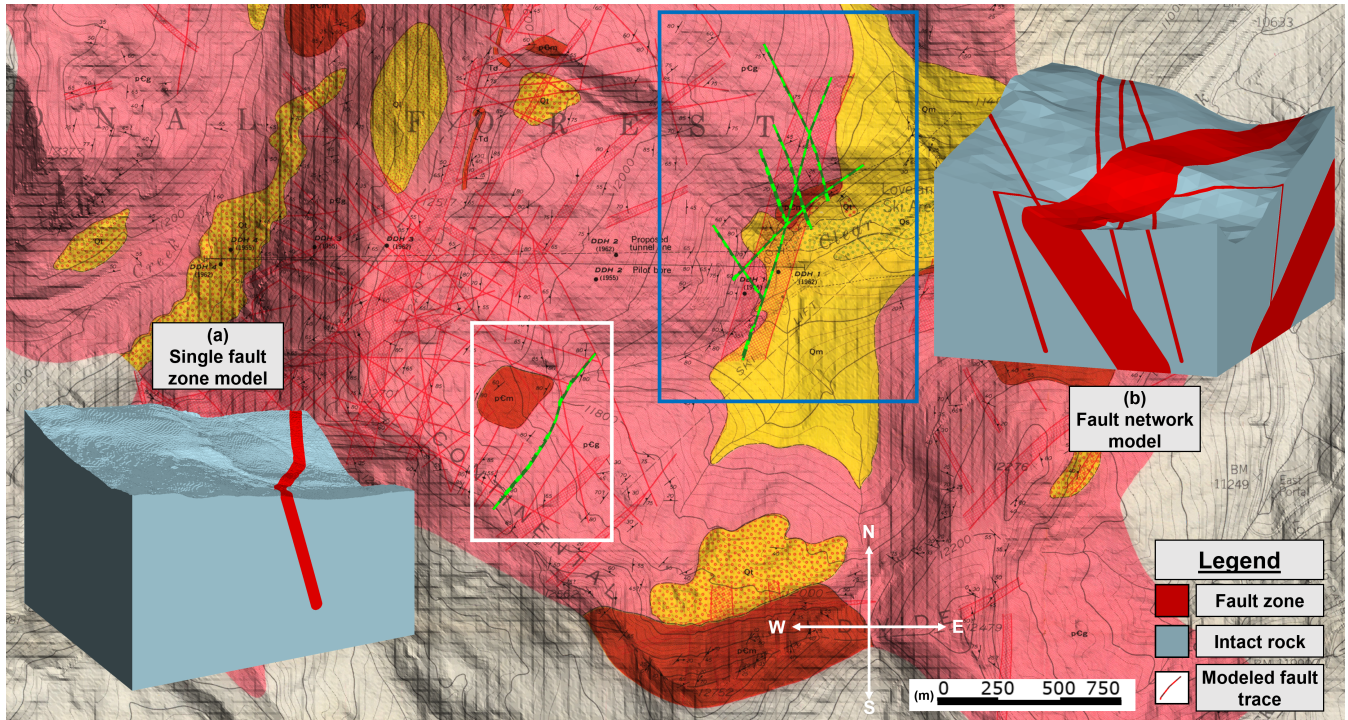


Figure 3. 1:12,000 geologic map from Robinson et al. (1974) showing mapped fault zones of varying widths. The white rectangle and associated overlay (a) show the single fault model while the blue rectangle and associated overlay (b) show the fault network model. Fault trace(s) used for modeling are highlighted within each rectangle as green polylines.

3.3 Figure 5

- legend is barely legible - please increase text size
- entropy plot of the fault zone thickness barely shows any uncertainty. If your discretization is not fine enough to resolve the simulated uncertainties, then is it worth incorporating into you model?

335 Authors' answer:

The legend text size has been increased to match the average text size of the paper's text.

340 The reviewer's comment is interesting and insightful, and is addressed briefly in the preceding section. While it is quite clear that the fault zone thickness uncertainty is largely insignificant in this single fault model (where the fault zone thickness was 8 m, vs. the 5 m block size), the authors observed that the wider fault zone present in the second, fault network model

would contribute more heavily to the model uncertainty. This reasoning, and the desire to present general recommendations to modeling the uncertainty of fault zones, led the authors to leave the results as is for the single fault model.

345 **Changes to the manuscript:**

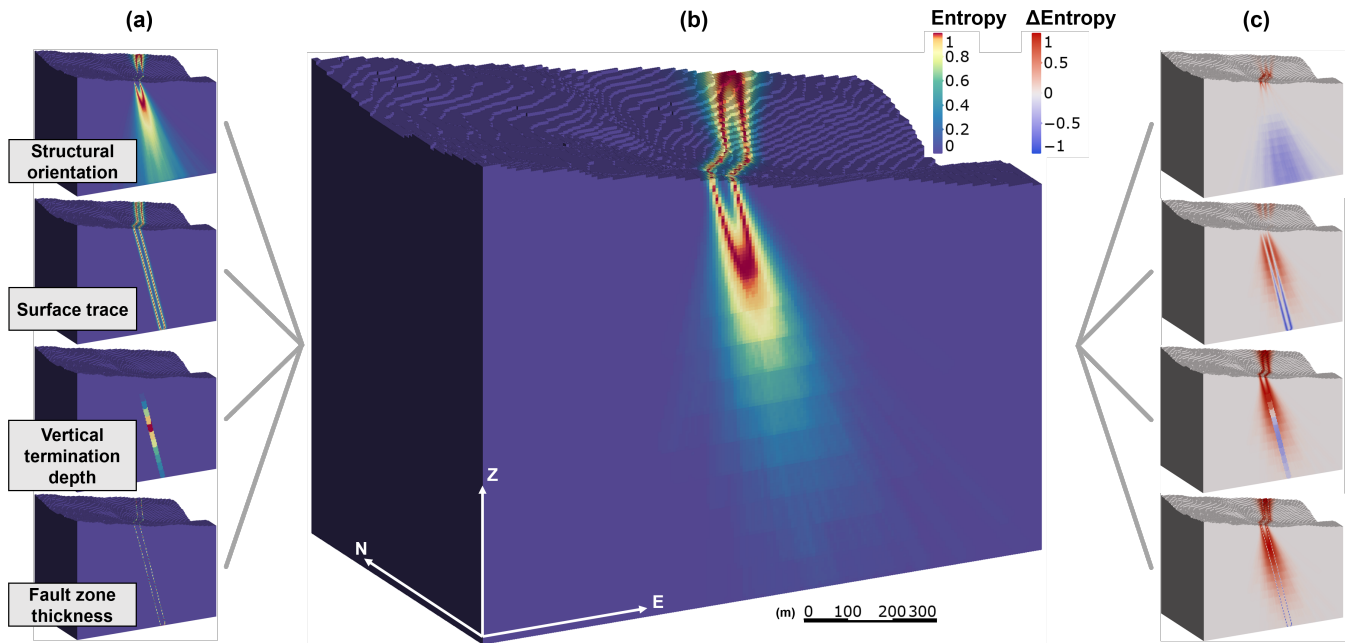


Figure 4. Block models showing information entropy quantified from (a) independent modeling inputs and (b) combined modeling inputs. The difference between the combined geologic model uncertainty and each independent modeling input is shown in (c), where blue values indicate that the independent modeling input showed greater entropy than the combined model uncertainty.

3.4 **Figure 6**

The use of trace plots is only useful if evaluating convergence of (e.g.) Markov chains. MCUP uses Monte Carlo simulation, thus the use of trace plots serves no purpose and is confusing. Also the rug plot on the left side shows the same information as the histogram of the vertical termination depth in the lower right. I'd recommend just using the histogram to demonstrate that you've sampled enough samples.

350

Authors' answer:

355 In line with this specific comment and the general comments above, the erroneous referrals to MCMC methods and the use of trace plots have been eliminated from the paper. They have been replaced by the appropriate discussion of assessing the exploration of the input uncertainty space using graphical representations of realizations and histograms of the Monte Carlo samples.

Changes to the manuscript:

360

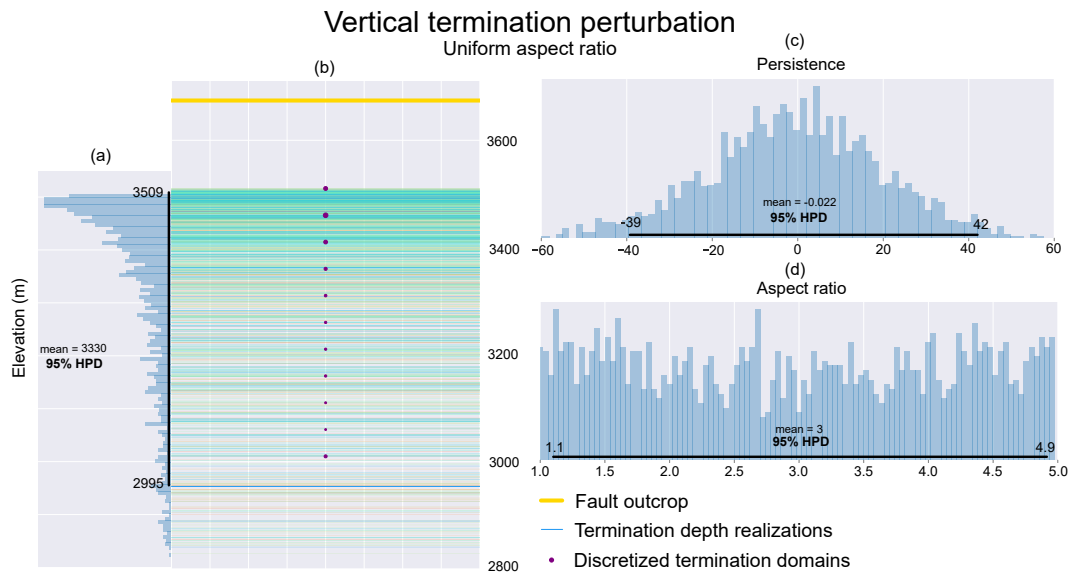


Figure 5. Realizations and Monte Carlo analysis results (trace plot and posterior histograms) **Visualization of Monte Carlo samples and associated geologic input realizations** from perturbation of the fault zone vertical termination depth based on a uniform distribution of fault aspect ratio. The 95% highest posterior predictive density is overlain on the posterior histograms of the Monte Carlo samples.

3.5 Figure 8

Authors' answer:

See above comment.

365

Changes to the manuscript:

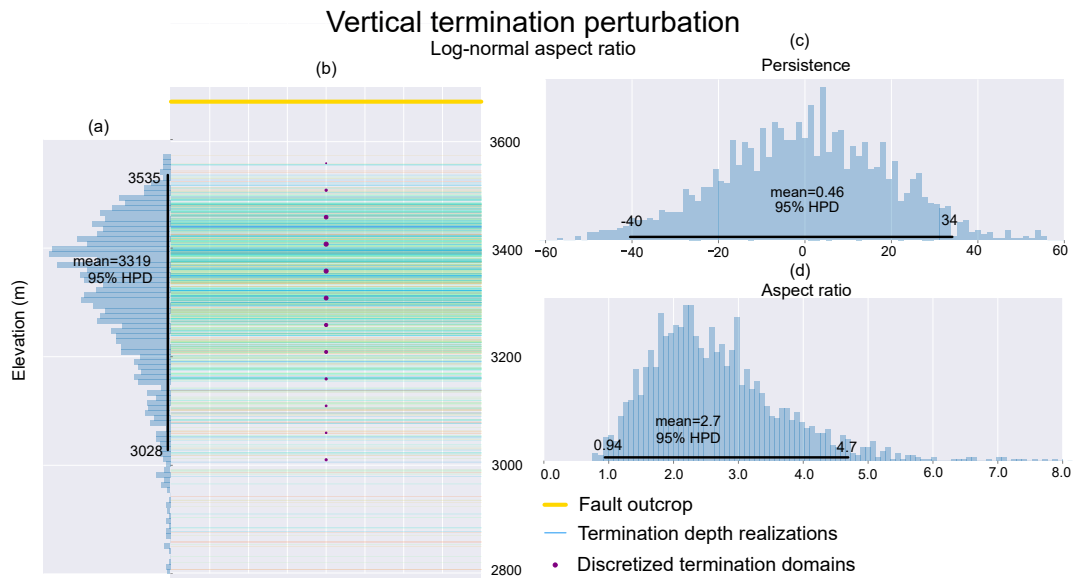


Figure 6. Realizations and Monte Carlo analysis results (trace plot and posterior histograms) **Visualization of Monte Carlo samples and associated geologic input realizations** from perturbation of the fault zone vertical termination depth, reparameterized using a log-normal distribution of fault aspect ratio. The 95% highest posterior predictive density is overlain on the posterior histograms of the Monte Carlo samples.

References

- Aydin, O. and Caers, J. K.: Quantifying structural uncertainty on fault networks using a marked point process within a Bayesian framework, *Tectonophysics*, 712–713, 101–124, <https://doi.org/10.1016/j.tecto.2017.04.027>, 2017.
- 370 Caine, J. S., Evans, J. P., and Forster, C. B.: Fault zone architecture and permeability structure, *Geology*, 24, 1025–1028, [https://doi.org/10.1130/0091-7613\(1996\)024<1025:FZAAPS>2.3.CO;2](https://doi.org/10.1130/0091-7613(1996)024<1025:FZAAPS>2.3.CO;2), 1996.
- Carmichael, T. and Ailleres, L.: Method and analysis for the upscaling of structural data, *Journal of Structural Geology*, 83, 121–133, <https://doi.org/10.1016/j.jsg.2015.09.002>, 2016.
- 375 Cherpeau, N. and Caumon, G.: Stochastic structural modelling in sparse data situations, *Petroleum Geoscience*, 21, 233–247, <https://doi.org/10.1144/petgeo2013-030>, 2015.
- Cherpeau, N., Caumon, G., and Lévy, B.: Stochastic simulations of fault networks in 3D structural modeling, *Comptes Rendus - Geoscience*, 342, 687–694, <https://doi.org/10.1016/j.crte.2010.04.008>, 2010.
- Childs, C., Manzocchi, T., Walsh, J. J., Bonson, C. G., Nicol, A., and Schöpfer, M. P.: A geometric model of fault zone and fault rock thickness variations, *Journal of Structural Geology*, 31, 117–127, <https://doi.org/10.1016/j.jsg.2008.08.009>, 2009.
- 380 Choi, J. H., Edwards, P., Ko, K., and Kim, Y. S.: Definition and classification of fault damage zones: A review and a new methodological approach, *Earth-Science Reviews*, 152, 70–87, <https://doi.org/10.1016/j.earscirev.2015.11.006>, 2016.
- de la Varga, M. and Wellmann, J. F.: Structural geologic modeling as an inference problem: A Bayesian perspective, *Interpretation*, 4, SM1–SM16, <https://doi.org/10.1190/INT-2015-0188.1>, 2016.
- 385 de la Varga, M., Schaaf, A., and Wellmann, F.: GemPy 1.0: Open-source stochastic geological modeling and inversion, *Geoscientific Model Development*, 12, 1–32, <https://doi.org/10.5194/gmd-12-1-2019>, 2019.
- Fisher, N., Lewis, T., and Embleton, B.: *Statistical analysis of spherical data*, Cambridge University Press, 1987.
- Fredman, N., Tveranger, J., Cardozo, N., Braathen, A., Soleng, H., Røe, P., Skorstad, A., and Syversveen, A. R.: Fault facies modeling: Technique and approach for 3-D conditioning and modeling of faulted grids, *AAPG Bulletin*, 92, 1457–1478, <https://doi.org/10.1306/06090807073>, 2008.
- 390 Krajnovich, A., Zhou, W., and Gutierrez, M.: Uncertainty Assessment of Fault Zones in 3D Geologic Models of Mountain Tunnels (in press), in: *Word Tunnel Congress, International Tunneling and Underground Space Association*, 2020.
- Manzocchi, T., Childs, C., and Walsh, J. J.: Faults and fault properties in hydrocarbon flow models, *Geofluids*, 10, 94–113, <https://doi.org/10.1111/j.1468-8123.2010.00283.x>, 2010.
- 395 Mardia, K. V. and Jupp, P. E.: *Directional Statistics*, John Wiley & Sons, London, <https://doi.org/10.1002/9780470316979>, 2000.
- Pakyuz-Charrier, E., Giraud, J., Ogarko, V., Lindsay, M., and Jessell, M.: Drillhole uncertainty propagation for three-dimensional geological modeling using Monte Carlo, *Tectonophysics*, 747–748, 16–39, <https://doi.org/10.1016/j.tecto.2018.09.005>, 2018a.
- Pakyuz-Charrier, E., Lindsay, M., Ogarko, V., Giraud, J., and Jessell, M.: Monte Carlo simulation for uncertainty estimation on structural data in implicit 3-D geological modeling, a guide for disturbance distribution selection and parameterization, *Solid Earth*, 9, 385–402, <https://doi.org/10.5194/se-9-385-2018>, 2018b.
- 400 Papadakis, M., Tsagris, M., Dimitriadis, M., Fafalios, S., Tsamardinos, I., Fasiolo, M., Borboudakis, G., Burkardt, J., Zou, C., and Lakiotaki, K.: Package ‘Rfast’, <https://rfast.eu>, 2018.
- Peacock, D. C., Nixon, C. W., Rotevatn, A., Sanderson, D. J., and Zuluaga, L. F.: Glossary of fault and other fracture networks, *Journal of Structural Geology*, 92, 12–29, <https://doi.org/10.1016/j.jsg.2016.09.008>, 2016.
- 405 Robinson, C. S., Lee, F. T., Scott, J. H., Carroll, R. D., Hurr, R. T., Richards, D. B., Mattei, F. A., Hartmann, B. E., and Abel, J. F.: Engineering Geologic, Geophysical, Hydrologic, and Rock-Mechanics Investigations of the Straight Creek Tunnel Site and Pilot Bore, Colorado, Tech. rep., United States Geological Survey, Washington, D.C., <https://doi.org/10.3133/pp815>, 1974.
- Røe, P., Georgsen, F., and Abrahamsen, P.: An Uncertainty Model for Fault Shape and Location, *Mathematical Geosciences*, 46, 957–969, <https://doi.org/10.1007/s11004-014-9536-z>, 2014.
- 410 Salvatier, J., Wiecki, T. V., and Fonnesbeck, C.: Probabilistic programming in Python using PyMC3, *PeerJ Computer Science*, 2, 1–24, <https://doi.org/10.7717/peerj-cs.55>, 2016.
- Schneeberger, R., de la Varga, M., Egli, D., Berger, A., Kober, F., Wellmann, F., and Herwegh, M.: Methods and uncertainty-estimations of 3D structural modelling in crystalline rocks: A case study, *Solid Earth*, 8, 987–1002, <https://doi.org/10.5194/se-2017-47>, 2017.
- Shipton, Z., Roberts, J., Comrie, E., Kremer, Y., Lunn, R., and Caine, J.: *Fault fictions : cognitive biases in the conceptualization of fault zones*, Geological Society Special Publications, 2019.
- 415 Torabi, A., Alaei, B., and Libak, A.: Normal fault 3D geometry and displacement revisited: Insights from faults in the Norwegian Barents Sea, *Marine and Petroleum Geology*, 99, 135–155, <https://doi.org/10.1016/j.marpetgeo.2018.09.032>, 2019a.
- Torabi, A., Johannessen, M. U., and Ellingsen, T. S. S.: Fault Core Thickness: Insights from Siliciclastic and Carbonate Rocks, *Geofluids*, 2019, 1–24, <https://doi.org/10.1155/2019/2918673>, 2019b.

- 420 Vollmer, F. W.: C program for automatic contouring of spherical orientation data using a modified Kamb method, 21, 31–49, [https://doi.org/10.1016/0098-3004\(94\)00058-3](https://doi.org/10.1016/0098-3004(94)00058-3), 1995.
- Zhong-Zhong, C.: The estimation of digitizing error and its propagation results in GIS and application to habitat mapping, Ph.D. thesis, University of Massachusetts Amherst, <https://scholarworks.umass.edu/dissertations/AAI9524686>, 1995.